10-2012

Rat Brain Pro-Oxidant Effects of Peripherally Administered 5 nm ceria 30 Days After Exposure

Sarita S. Hardas
University of Kentucky, saritash135@gmail.com

Rukhsana Sultana
University of Kentucky, rsult2@uky.edu

Govind Warrier
University of Kentucky

Mo Dan
University of Kentucky, mo.dan@uky.edu

Rebecca L. Florence
University of Kentucky

See next page for additional authors

Rat Brain Pro-Oxidant Effects of Peripherally Administered 5 nm ceria 30 Days After Exposure

Digital Object Identifier (DOI)
https://doi.org/10.1016/j.neuro.2012.06.007

Notes/Citation Information
Published in *NeuroToxicology*, v. 33, issue 5.

Authors
Sarita S. Hardas, Rukhsana Sultana, Govind Warrier, Mo Dan, Rebecca L. Florence, Peng Wu, Eric A. Grulke, Michael T. Tseng, Jason M. Unrine, Uschi M. Graham, Robert A. Yokel, and D. Allan Butterfield

Rat brain pro-oxidant effects of peripherally administered 5 nm ceria 30 days after exposure

Sarita S. Hardas*, Rukhsana Sultana*, Govind Warrier*, Mo Dan[‡], Rebecca L. Florence[‡], Peng Wu[III], Eric A. Grulke[III], Michael T. Tseng[IIII], Jason M. Unrine[¶], Uschi M. Graham[||], Robert A. Yokel[‡, §] and, D. Allan Butterfield *[, †]

Sarita S. Hardas: *Department of Chemistry, University of Kentucky, Lexington, Kentucky 40506-0055. Email: Sarita.Hardas@uky.edu

Rukhsana Sultana: *Department of Chemistry, University of Kentucky, Lexington, Kentucky 40506-0055. Email: rsult2@uky.edu

Govind Warrier: *Department of Chemistry, University of Kentucky, Lexington, Kentucky 40506-0055. Email: govind.warrier@uky.edu

Mo Dan: ‡Department of Pharmaceutical Sciences, University of Kentucky Academic Medical Center, University of Kentucky, Lexington, Kentucky 40536-0082. Email: mo.dan@uky.edu

Rebecca L. Florence: ‡Department of Pharmaceutical Sciences, University of Kentucky Academic Medical Center, University of Kentucky, Lexington, Kentucky 40536-0082. Email: rlstep2@uky.edu

Peng Wu: IIIChemical and Materials Engineering Department, University of Kentucky, Lexington, Kentucky 40506-0503. Email: peng.wu@uky.edu

Eric Grulke: IIIChemical and Materials Engineering Department, University of Kentucky, Lexington, Kentucky 40506-0503. Email: eric.grulke@uky.edu

Michael T. Tseng: IIIIDepartment of Anatomical Sciences & Neurobiology, University of Louisville, Louisville, Kentucky 40202. Email: mttsen01@louisville.edu

Jason M. Unrine: ¶Department of Plant and Soil Sciences, University of Kentucky, Lexington, Kentucky 40546-0091. Email: jason.unrine@uky.edu

Uschi M. Graham: IICenter for Applied Energy Research, University of Kentucky, Lexington, Kentucky 40511. Email: uschi.graham@uky.edu

Robert A. Yokel: ‡Department of Pharmaceutical Sciences, University of Kentucky Academic Medical Center, University of Kentucky, Lexington, Kentucky 40536-0082, § Graduate Center for Toxicology, University of Kentucky Academic Medical Center, Lexington, Kentucky 40506-9983. Email: ryokel@email.uky.edu

D. Allan Butterfield: *Department of Chemistry, University of Kentucky, Lexington, Kentucky 40506-0055, †Center of Membrane Sciences, University of Kentucky, Lexington, Kentucky 40506-0059. Email: dabcns@uky.edu

Corresponding author:

D. Allan Butterfield, Ph.D.

Department of Chemistry,

University of Kentucky,

Lexington,

Kentucky 40506-0055,

Phone: 859-257-3184

Fax: 859-323-1069

Email: dabcns@uky.edu

Short title: Nanoceria pro-oxidant effect on brain

Abbreviations:

3NT	protein bound 3-nitrotyrosine
Ce	cerium
Cat	catalase
EELS	electron energy loss spectroscopy
ENM	engineered nanomaterial
GR	glutathione reductase
GPx	glutathione peroxidase
H_2O_2	Hydrogen peroxide
Hsp70	heat shock protein 70
HNE	protein-bound 4-hydroxy-2-trans-nonenal
ICP-MS	inductively coupled plasma mass spectrometry
iNOS	inducible nitric oxide synthase
MDL	method detection limit
PC	protein carbonyl
ROS	reactive oxygen species
RNS	reactive nitrogen species
SOD	superoxide dismutase
TEM	transmission electron microscopy

Abstract:

The objective of this study was to determine the residual pro-or anti-oxidant effects in rat brain 30 days after systemic administration of a 5 nm citrate-stabilized ceria dispersion. A ~4% aqueous ceria dispersion was iv-infused (0 or 85 mg/kg) into rats which were terminated 30 days later. Ceria concentration, localization, and chemical speciation in the brain was assessed by inductively coupled plasma mass spectrometry (ICP-MS), light and electron microscopy (EM), and electron energy loss spectroscopy (EELS), respectively. Pro- or anti-oxidant effects were evaluated by measuring levels of protein carbonyls (PC), 3-nitrotyrosine (3NT), and protein-bound-4-hydroxy-2-trans-nonenal (HNE) in the hippocampus, cortex, and cerebellum. Glutathione reductase (GR), glutathione peroxidase (GPx), superoxide dismutase (SOD), and catalase levels and activity were measured in addition to levels of inducible nitric oxide (iNOS), and heat shock protein-70 (Hsp70). The blood brain barrier (BBB) was visibly intact and no ceria was seen in the brain cells. Ceria elevated PC and Hsp70 levels in hippocampus and cerebellum, while 3NT and iNOS levels were elevated in the cortex. Whereas glutathione peroxidase and catalase activity were decreased in the hippocampus, GR levels were decreased in the cortex, and GPx and catalase levels were decreased in the cerebellum. The GSH: GSSG ratio, an index of cellular redox status, was decreased in the hippocampus and cerebellum. The results are in accordance with the observation that this nanoscale material remains in this mammal model up to 30 days after its administration and the hypothesis that it exerts pro-oxidant effects on the brain without crossing the BBB. These results have important implications on the potential use of ceria ENM as therapeutic agents.

Key words: oxidative stress; ceria; brain; neurotoxicity; nanomaterial, nanoparticles; rat**.**

Introduction:

Engineered nanomaterials (ENM) can be manufactured in a variety of shapes and sizes and physico-chemical, surface, as well as optical and magnetic properties. ENMs have numerous applications in research, medicine, electronics and other industries. Physico-chemical properties of nanomaterials differ from their bulk forms mainly because of the larger surface area to mass ratio, which affects reactivity, strength and electrical properties of nanomaterials. Because of their comparable size with biological molecules like proteins and DNA, ENMs can gain access to usually difficult to reach biological compartments in cells (Fubini et al. 2010). Increased surface activity can facilitate interactions with biological molecules, which may evoke greater physiological responses, different from the same basic material with larger particle size, the bulk form equivalent of ENMs (Donaldson et al. 2004; Landsiedel et al. 2009; Xia et al. 2009). One effect exhibited by ENMs is the generation of free radicals or induction of oxidative stress, which is also a primary mechanism of ENM toxicity (Xia et al. 2009). Oxidative stress effects are direct consequences of imbalance in the rates of reactive oxygen and / or nitrogen species (ROS or RNS) production verses scavenging of ROS and / or RNS and / or antioxidant levels (Butterfield et al. 2007).

Ceria ENM (a.k.a. cerium oxide; CeO_2), which is one of the most used ENM employed in different industrial applications (Yokel et al. 2009; Hardas et al. 2010) has been shown to have both anti-inflammatory properties as well as potent toxicity. However, there is no clear understanding of what exactly controls ceria's pro-or anti-oxidant effects. A recently published report summarizes findings of *in vitro* and *in vivo* studies conducted with ceria ENM under basal and induced oxidative stress conditions (Celardo et al. 2011). Ceria exhibited antioxidant properties evidenced by scavenging free radicals, by reducing levels of peroxides, iNOS, TNF-α, NF-κβ, and interleukin, by promoting cell viability or protecting organelles from diesel exhaust and cigarette smoke-induced oxidative stress, ROS generating chemical agents, or side effects

of radiation treatment. Ceria has been suggested for potential use in the treatment of diabetic cardiomyopathy, cancer, stroke, retinal degradation and Alzheimer's disease as well as to prolong life span (Chen et al. 2006; Rzigalinski et al. 2006; Das et al. 2007; Xia et al. 2008; D'Angelo et al. 2009; Hirst et al. 2009; Babu et al. 2010; Colon et al. 2010; Younce et al. 2010; Estevez et al. 2011; Niu et al. 2011). Antioxidant properties of ceria may be related to its SOD- and catalase-mimicking activity (Korsvik et al. 2007; Pirmohamed et al. 2010) attributed to Ce3+/ Ce4+ redox coupling (Celardo et al. 2011). In contrast, there are reports of ceria induced pro-oxidant effects under basal conditions. In different cell culture studies, ceria ENM mediated ROS injury, induced lipid peroxidation, caused membrane damage, led to elevation of the cytokine, IL-8, led to depletion of GSH, and led to reduced cell viability (Brunner et al. 2006; Lin et al. 2006; Park et al. 2008; Auffan et al. 2009).

To utilize ceria for therapeutic and non-therapeutic applications, it is important to know the long term effects of intended and un-intended ceria exposure on mammals. Most reports on effects of ceria ENM were conducted using non-mammalian organisms or in cell culture, and none of these addressed long-term effects or fate of ceria. In addition to our own previous studies (Yokel et al. 2009; Hardas et al. 2010), a few ceria ENM studies were conducted in intact animals (Chen et al. 2006; Niu et al. 2007; Hirst et al. 2009; Amin et al. 2011; Choi et al. 2011; Hirst et al. 2011; Srinivas et al. 2011; Zhou et al. 2011). One study reports that deposition and retention of ceria in various vital organs and increased WBC count were seen 30 days after intraperitoneal and intravenous injection to mice, but otherwise ceria was tolerated by animals (Hirst et al. 2011). Ceria reduced myocardial oxidative stress in transgenic mice for ischemic cardiomyopathy, rat liver from monocrotaline-induced ROS injury by induction of GSH levels and intravitreal injections of ceria inhibited retinal neovascular lesions (Niu et al. 2007; Amin et al. 2011; Zhou et al. 2011). However, after pulmonary inhalation of ceria ENM, granulomatous pathology and GSH depletion were seen in rat lungs (Cho et al. 2010; Srinivas et al. 2011).

Animal studies have also reported that ceria ENM can accumulate in various organs, including the heart and lung, irrespective of the point of entry or distance (from injection point and organ specifically examined) when supplied as intravenous or intra-peritoneal injections or as a food additive (Chen et al. 2006; Niu et al. 2007; Hirst et al. 2009). This accumulation may lead to systemic effects involving the inflammatory response (Celardo et al. 2011) or increased ROS production under normal physiological conditions (Hirst et al. 2011).

To our knowledge there is no prior information available on the long-term effects (30 d or more after administration) of ceria on brain and how these effects may contrast with an immediate response after the initial ENM contact. Our previous study showed moderate pro-oxidant effects on rat brain, 1 and 20 h after a single acute systemic instillation of 5 nm ceria ENM (Hardas et al. 2010). The current study discusses residual effects of oxidative stress parameters in brain 30 days after one single acute ENM peripheral administration using 5 nm ceria ENM. To address the objective, the levels and activities of the antioxidant enzymes catalase, manganese superoxide dismutase (Mn-SOD), glutathione peroxidase (GPx), and glutathione reductase (GR), were measured along with the ratio of reduced glutathione (GSH) to its oxidized form (GSSG). To understand the extent of changes in cellular redox status, the levels of oxidative stress endpoints, protein carbonyl (PC), 3-nitrotyrosine (3NT), and protein bound 4- hydroxyl-2-trans nonenal (HNE), were measured along with heat shock protein (Hsp70) levels.

Materials and Methods:

All the materials, methods including the well characterized 5 nm ceria ENM are same as that used in our recently published study (Hardas et al. 2010). The rats used are of the same strain, sex and approximately same weight as that used in the previous study with 5 nm ceria ENM (Hardas et al. 2010). Therefore, only a brief overview is presented.

Nanomaterial:

Cerium chloride heptahydrate (Sigma-Aldrich # 228931, 99.9% metal basis), ammonium hydroxide (Fisher #3256, ACS, 28-30%) and citric acid monohydrate (EMD Chemicals Inc # CX1725-1, GR ACS) were used without further purification. A hydrothermal method was used to synthesize ~5nm ceria aqueous suspension. Briefly, a 20 ml aqueous mixture of 0.01 mol cerium chloride and 0.01 M citric acid was added to 20 ml of 3 M ammonium hydroxide. After stirring for 24 h at 50°C, the solution was transferred into a Teflon-lined stainless steel bomb and heated at 80°C for 24 h to complete the reaction. The final dispersion of ceria ENM was infused intravenously to the rats over 1 h without any further treatment or purification.

Ceria characterization:

The details of ceria ENM characterization are published in our earlier study (Hardas et al. 2010). In brief, the morphology and crystallinity of the ceria was evaluated using a 200-keV field emission analytical transmission electron microscope (JEOL JEM-2010F, Tokyo, Japan) equipped with an Oxford energy dispersive X-ray spectrometer. The particle size distributions (PSDs) were determined using dynamic light scattering (DLS: Brookhaven Instruments Corporation, 90Plus NanoParticle Size Distribution Analyzer, Holtsville, NY, USA). The surface area of the dried ceria powder was determined using a BETASAP 2020 surface area analyzer that determines particle surface area based on nitrogen adsorption (Micromeritics Instrument Corporation, Norcross, GA, USA). The ceria content of the dispersion and the potential presence of contaminating elements/metals were determined by digestion of ceria dispersion samples and analysis by ICP-MS. Electron energy loss spectroscopy (EELS) was performed on rat liver tissue using a JEOL 2010F STEM outfitted with a URP pole piece, GATAN 2000 GIF (Pleasanton, CA, USA), GATAN DigiScan II, Fischione HAADF STEM detector (Export, PA, USA), and EmiSpec EsVision software (Tempe, AZ, USA).

Animals:

In the current study 16 male Sprague Dawley rats, weighing 328 ± 21 g (mean ± SD), were obtained from Harlan, Indianapolis, IN, and were housed individually prior to study and after cannulae removal (a few days after the iv infusion) in the University of Kentucky Division of Laboratory Animal Resources facility under a 12:12 h light:dark cycle at 70 ± 8°F and 30 to 70% humidity. The rats had *ad lib* access to 2018 Harlan diet and RO water. All procedures involving animals were approved by the University of Kentucky Institutional Animal Care and Use Committee. The research was conducted in accordance with the Guiding Principles in the Use of Animals in Toxicology (http://www.toxicology.org/ai/air/air6.asp)..

Ceria administration:

Rats were prepared with 2 cannulae that terminated in the vena cava to administer the ceria dispersion or water (controls) in one and 1.8% sodium chloride in the second, to avoid agglomeration induced by sodium chloride or 10% sucrose, which are commonly added to prepare iso-osmotic solutions (Yokel et al. 2009); (Hardas et al. 2010). Seven rats received 0 and nine rats received 85 mg ceria/kg as a single acute dose of ENM. The rats were terminated 30 days after the infusion. Post-mortem samples including brain cortex, hippocampus, and cerebellum were harvested rapidly and were frozen in liquid nitrogen and stored at -80 ^{0}C for later oxidative stress measurements. Cerium concentrations in brain cortex, blood, and liver were analyzed by ICP-MS; Agilent 7500cx, (Santa Clara, CA, USA) after microwave digestion as described previously (Hardas et al., 2010). The detection limits of this method were 0.089 mg Ce/kg. Mean spike recovery ranged from 97 to 105%. Relative percent difference between replicates was ≤ 2% for 30-120 ng Ce/ml and 18% for 1.5 ng Ce/ml.

Light and electron microscopic assessment:

After animal termination brains were removed, sliced coronally in a brain matrix (Braintree acrylic matrix BS-A 6000C). Sections containing hippocampus were fixed by immersion in 4%

buffered formalin. Cerebellum was similarly sliced and fixed. Samples were cut into 3 mm cubes, dehydrated and embedded in Araldite 502. After polymerization, one micron thick sections were cut and stained with toluidine blue for LM examination. Selected blocks were sectioned at 80 nm, collected on 200 mesh copper grids and examined in a Philips CM 10 electron microscope at 60 kV.

Oxidative stress assessment, sample preparation:

All sample preparation and protein assays were carried out as described in our previous publication (Hardas et al. 2010). Each sample was individually thawed and homogenized using a 550 sonic dismembrator from Fischer Scientific for 10 to 20 s on ice. The buffer used for homogenization contained 0.32 M sucrose, 0.125 M Tris, 0.6 mM $MgCl_2$, and protease inhibitors (4 µg/ul leupeptin, 4 µg/ul pepstatin A, 5 µg/ul aprotinin, and 0.2 mM phenylmethylsulfonyl fluoride) at pH 8.0. Total protein concentration for each sample was measured using the bicinchoninic acid assay and equal amounts of protein from control and treated samples were used in each assay.

Oxidative stress markers:

The oxidative stress markers PC, 3NT, and HNE were assessed for each homogenized sample using the slot blot technique. Specific antibodies were used to determine the levels of PC, 3NT, HNE in controls and treated samples as previously described (Hardas et al. 2010).

GSH and GSSG levels:

The reduced (GSH) and oxidized glutathione (GSSG) levels were simultaneously measured in each sample as previously described (Hissin and Hilf 1976). A small amount of brain tissue was rapidly weighed, homogenized with metaphosphoric acid (25%) and sodium phosphate (0.1 M) - ethylenediaminetetraacetic acid (0.005 M) buffer (pH 8) and then centrifuged. For GSH levels,

an aliquot of supernatant was further diluted with phosphate buffer and then incubated with o-phthaldehyde (OPT), before determination of fluorescence (λ excitation 350 nm and emission 420 nm). For GSSG levels equal volumes of supernatant were incubated with N-ethylmaleimide (0.04 M) for 30 min and then diluted with sodium hydroxide (0.1 N), before assaying with OPT. The GSH to GSSG ratio for each sample was calculated by comparing the fluorescence values from each assay to their respective calibration curves. The final values are % control of mean ± SEM of treated vs. control samples.

Western blot analysis:

The levels of the antioxidant enzymes GR, GPx, MnSOD, catalase, Hsp70 and iNOS were measured using immunoblotting-Western blot techniques as described in our earlier publications (Sultana et al. 2008; Hardas et al. 2010). In brief, 75 µg protein from each homogenized sample was loaded and separated on SDS-PAGE alongside its respective control. The separated proteins were transferred from poly-acrylamide gels to nitrocellulose membranes, and then the band of specific protein identified using a specific antibody against that protein. The band-intensity was quantified as previously described (Hardas et al., 2010) by using the image analysis software, ImageQuant, purchased from GE Healthcare.

Enzyme activity assays:

The activities of GR, GPx, MnSOD and catalase enzymes were measured as described earlier (Hardas et al. 2010), with commercially available kits from Cayman Chemical Company, Ann Arbor, MI, USA as per the manufacturer's instructions. Suitable protein samples from each organ (i.e., 10-20 µg for brain homogenate) were mixed with assay buffer and with other specific reagents for each assay on 96-well plates. Enzymatic reactions were initiated by addition of reaction initiator reagents, NADPH for GR, cumene hydroperoxide for GPx, xanthine oxidase for SOD, and hydrogen peroxide for the catalase assay. Progression of the each reaction was

studied separately by spectrophotometry at 340 nm (for GR and GPx), at 460 nm (for SOD) and at 540 nm (for catalase).

Data and statistical analysis:

The slot blot, Western blot and enzyme assay results are presented as mean ± SEM. The control mean was normalized to 100%. Grubb's test was used to identify outliers in oxidative stress parameter results. Student's unpaired t-test was used to evaluate significant difference between controls and ceria treated samples. Subsequently, two-way ANOVA was conducted to determine the differential effect of ceria ENM treatment among the three brain regions studied. Significance was accepted at $p < 0.05$.

Results:

Ceria composition

HR-TEM/HR-STEM showed the ceria ENM was polyhedral shaped (Figure 1). The XRD patterns demonstrated the ceria was highly crystalline, with face centered cubic unit cells with corresponding Miller indices of the most common faces of (111), (210) and (200). Evaluation of a number of TEM images showed that the ceria had a number-average primary particle size of ~5 nm. The ceria ENM surface area was 121 m^2/g, assuming the density of a ceria nanoparticle 7600 kg/m^3 (the bulk density), the back-calculated average diameter should be 6.5nm that fits our TEM observation quite well. Analysis by ICP-MS of the ceria dispersion used showed that the ceria content of the as-synthesized dispersion was 4.35 ± 0.20% and the free cerium ion content was 11.6 ± 0.3%.

Dispersion properties

The citrate ion was found to be a stabilizing electrolyte for ceria nanoparticles. At pH below 7.0 the ceria agglomerated; therefore, the ceria was maintained as an aqueous dispersion at pH 7.7 to 8. Zeta potential of the citrate-stabilized particles was -53 ± 7 mV at pH ~ 7.35 (Hardas et al. 2010). In general, dispersions with absolute values of zeta potential greater than 30 to 40 mV

are expected to be stable, and the stability of dispersion is better with higher zeta potential. The cerium concentration in samples taken from the top and bottom of two ceria dispersion samples in covered 15 ml centrifuge tubes that were un-disturbed for > 2 months were within 2.5% of each other, demonstrating dispersion stability (data not shown).

Ceria concentration in brain and electron micrography

ICP-MS analysis showed that a very small amount of ceria was present in the brain compared to the liver (Table 1). Electron micrographic studies suggested that ceria ENM was not present in the brain, but located on the luminal side of the blood brain barrier (BBB) endothelium. The hippocampus and cerebellum tissues did not show obvious ceria induced injury as no necrotic neurons or elevated gliosis were observed and the BBB was visibly intact (data not shown).

EELS results

Electron energy loss spectroscopic (EELS) measurements on liver tissue were performed as a representative organ. The 5 nm ceria agglomerates were located in the tissue 30 days after infusion into rats. The ratio of Ce(3+) to Ce(4+) was evaluated using EELS measurements *in vivo* 30 days post infusion. Further, this ratio was compared with the ratio of Ce^{3+}/Ce^{4+} obtained in freshly synthesized ceria. The high Ce^{3+}/ Ce^{4+} ratio that was obtained in the as-synthesized, fresh 5 nm ceria particles seems to have only been altered slightly in individual ceria measured in liver after 30 days *in vivo*. However, this difference was not significant (data not shown).

Oxidative Stress Indices

The primary aim of these studies was to evaluate indices of oxidative stress in brain 30 days following a single ceria ENM administration.

Ceria treatment affected catalase levels and activities

Previously ceria ENM was reported to have a H_2O_2-producing ability (Korsvik et al. 2007); therefore, the effect of 5 nm ceria ENM on levels and activity of a primary H_2O_2-reducing enzyme (catalase) was determined in the present study. Catalase activity was significantly decreased in the hippocampus (~18%, *p<0.05, Figure 2b) and catalase levels were significantly decreased in the cerebellum (~16%, *p<0.05, Figure 4a). To determine the influence of ceria treatment on the SOD enzyme or contribution to H_2O_2 levels from SODs, if any, the level of MnSOD and its activity were measured. There were no significant changes observed in the levels or activity of MnSOD (data not shown).

Ceria treatment decreases GPx levels, activity and the GSH-GSSG ratio

GPx reduces H_2O_2 along with other peroxides using glutathione (GSH) as a source of reducing equivalents. The activity of GPx was significantly decreased in the hippocampus (~69%, **p<0.001, Figure 2b) and in cerebellum (~23 %, *p<0.05, Figure 4b). GPx levels showed a decreasing trend in all brain regions, but was significantly decreased only in cerebellum (~27 %, *p<0.05, Figure 4a). Within the three brain regions examined, hippocampal GPx activity was significantly inhibited compared to that in cortex and cerebellum (**p < 0.01). GR levels were significantly decreased (~24%, *p<0.05, Figure 3a) in the cortex. GR activity did not show any significant change in any of the three brain regions studied. A marker of overall cellular redox status was evaluated by comparing the GSH:GSSG ratio of ceria-treated samples. The GSH: GSSG ratio was significantly decreased in the hippocampus (~13%, *p<0.05, Figure 2b) and cerebellum (~15%, **p<0.01, Figure 4b) consistent with an increase in oxidative stress.

Ceria treatment induced protein oxidation

The levels of PC showed a significant increase in the hippocampus (~ 19%, *p<0.05, Figure 2c) and cerebellum (~12 %, *p<0.05, Figure 4c) in treated vs. control samples. 3NT levels were significantly increased in the cortex (~20%, *p<0.05, Figure 3c). There was no significant

change in protein-bound HNE levels in any of the three brain regions examined. Consistent with increased 3NT levels in cortical region, iNOS levels were increased significantly (~27%, *p<0.05, Figure 3d), and there was a positive correlation between 3NT and iNOS levels (r= 0.67, p < 0.05, Figure 3d).

Hsp-70 levels increased after ceria treatment

Hsp-70 is a member of the heat shock protein family and inducible by oxidative stress. Hsp-70 levels were significantly increased in the hippocampus (~49%, *p<0.05, Figure 2a), as well as compared to that of cortical and cerebellar Hsp70 levels (*p<0.05). In the cerebellum Hsp70 levels were increased (~40% *p<0.05, Figure 4a). These results are consistent with diminution of GSH levels indicated by the decreased GSH: GSSG ratio in these brain regions.

Discussion:

The present work was conducted to evaluate the oxidative stress effects of ceria ENM in brain 30 d after a single acute peripheral administration of 5 nm ceria ENM. ROS and RNS are inevitable byproducts of all major metabolic cellular processes and conspicuous by their high reactivity and high cytotoxicity. Apart from being a cause for many pathological conditions or cellular disturbances, ROS/ RNS also play important roles in cell signaling pathways and cellular homeostasis (Celardo et al. 2011; Butterfield et al., 2001). Therefore, balancing excessive and insufficient ROS/RNS is critical, and endogenous enzymes like GPx, GR, catalase and SOD as well as antioxidants like glutathione maintain this redox balance efficiently. Any perturbation to this redox balance causes oxidative stress. One of the mechanisms by which nanomaterials induce toxicity is by inducing ROS production, elevating oxidative stress, which damages proteins, lipids or DNA (Butterfield and Stadtman, 1997; Nel et al. 2006; Sharma Sharma 2007; Mocan et al. 2010).

Owing to its redox switching between two oxidation states, 3+ and 4+, ceria exhibits catalytic activity, which has made it useful in industrial applications (Celardo et al. 2011). Ceria's surface redox capability can affect the immediate surroundings and has been strongly linked to particle size (Gilliss et al. 2005). The characteristic oxidation and reduction in ceria ENM is linked to the continued possibility to absorb and release oxygen by inducing oxygen vacancies close to the particle surface. The Ce^{3+}/ Ce^{4+} valance switch resembles redox behavior of some biological antioxidant enzymes like SOD and catalase. The high Ce^{3+}/ Ce^{4+} ratio is responsible for the ceria ENM SOD-mimetic activity (Korsvik et al. 2007).

In our previous study, the same 5 nm ceria ENM at the same dose as used in the present study showed moderate effects, on brain redox status, while catalase levels and activities were increased in hippocampus after 1 and 20 h, respectively, and catalase activity was decreased in cerebellum after 1 h. No change was seen in PC, 3NT and HNE levels (Hardas et al. 2010). Although, ceria ENM was not found in the brain, but located on the luminal side of the BBB endothelial cells and the BBB was intact, the current study demonstrated that 5 nm ceria ENM produced significant pro-oxidant effects in the brain 30 days following administration and their retention in peripheral organs (Figure 5). Based on the EELS analysis, it would appear that even after a long-term exposure time of 30 days ceria continued to show a significant +3 valence on the surface. Similar high +3 valence was observed on surface of ceria ENM after short-term retention inside the rat, as seen in our previous study (Hardas et al. 2010), which was not significantly different compared to freshly prepared ceria. This finding clearly defines an enhanced oxygen storage capacity (Nesic et al.) of the ceria surfaces that does not diminish greatly throughout the 30 day exposure period. Yet, ceria with enhanced OSC was shown in the current study to have a significant pro-oxidative effect in the brain after the long-term exposure following a single administration.

As depicted in Figure 5, a decline in the GSH: GSSG ratio (in hippocampus and cerebellum) in the current study indicates elevated oxidative stress in the cellular environment. A similar observation was reported in Park *et. al.* in which 30 nm ceria depleted GSH levels in human lung epithelial cells in a dose-dependent manner (Park et al. 2008). Hydroxylated derivatives of fullerenes also decreased the GSH: GSSG ratio and induced lipid peroxidation (Nakagawa et al. 2011). At the cellular level the GSH: GSSG ratio is dependent on GPx and GR enzymes, and in the current study we observed decreased GPx activity (in hippocampus and cerebellum), decreased GPx levels (in cerebellum) and decreased GR levels (cortex). Similarly, 15 nm silver and 90 nm copper ENM down-regulated GPx gene expression (Wang et al. 2009), 25 nm silver ENM (Rahman et al. 2009) and SWCNT (Wang et al. 2011) inhibited GPx activity, and silica ENM reduced GR activity (Akhtar et al. 2010). Thus it may be possible that after 30 days following administration, ENM have deleterious effects on enzymes needed for maintenance of the reduced thiol status of the cells (Figure 5).

Figure 5 also shows that inhibition of catalase and GPx activities may lead to accumulation of H_2O_2 and ultimately increased production of hydroxyl radicals (OH•). Activity of catalase can be inhibited by hydroxyl radicals (OH•) and that of GPx by H_2O_2 and hydroperoxides (Pigeolet et al. 1990). Ceria ENM can produce H_2O_2 under abiotic conditions (Korsvik et al. 2007; Xia et al. 2008), and H_2O_2 has high membrane permeability (Halliwell 1992). Further H_2O_2 can undergo a Fenton-type reaction to produce highly potent OH• radicals as noted above (Figure 5). A lack of change in SOD activity and level in the current study may imply that endogenous SOD does not account for ceria-induced elevated oxidative stress in brain. Therefore, ceria ENM treatment may have caused induction in ROS that led to oxidative inhibition of antioxidant enzyme activities, decreased the GSH: GSSG ratio and increased in PC and 3NT levels observed in the present study. Similar consequences of oxidative stress were seen after exposure to various

other ENM, such as TiO_2 (Hao et al. 2009; Liang et al. 2009; Xiong et al. 2011), SWCNT(Wang et al. 2011), MWCNT(Guo et al. 2011), hematite (Radu et al. 2010), and ZnO (Xia et al. 2008).

The elevated 3NT levels, a marker for increased nitrosive stress, are consistent with elevated levels of inducible nitric oxide synthase (iNOS). iNOS exists at extremely low levels under normal physiological conditions, but it is inducible by endotoxin and inflammatory cytokines among other stresses (Calabrese et al. 2000). We found a correlation between 3NT levels and iNOS levels in the cortical region of rats examined 30 d after ceria ENM treatment. It may indicate that increased 3NT levels are due to increased NO production in the cortex and we speculate that iNOS levels concurrently may be induced following ceria treatment via increased cytokine production.

Electron micrograph analysis showed an intact BBB and an absence of any significant amount of ceria in the brain. However, cobalt-chromium ENMs have damaged DNAs without crossing cellular membranes (Bhabra et al. 2009), and the chemotherapeutic drug doxorubicin led to neurotoxic effects without ever crossing the BBB (Tangpong et al. 2006). Similarly, it is conceivable that the observed oxidative stress response in brain regions could be due to the accumulation of 5 nm ceria in peripheral organs and subsequent elevation of BBB-permeable inflammatory cytokines. Studies to test this notion are in progress.

Induction of heat shock protein Hsp-70 levels as seen in the present study is in agreement with other literature reports. Similar to effects of silver ENM (Ahamed et al. 2010) and fullerene C60 (Usenko et al. 2008) treatments, Hsp-70 levels and other oxidative stress markers were induced with concomitant decrease in the GSH: GSSG ratio. In a transgenic mouse model for cardiomyopathy, Hsp-70 levels were increased as an oxidative stress marker of ER stress. Ceria ENM treatment rescued these cells from ER stress and as a result Hsp-70 expression

was down regulated (Niu et al. 2007). In the present study, 5 nm ceria ENM indirectly induced ROS production in brain causing depletion of GSH, which initially induces antioxidant levels but over 30 days eventually inhibits H_2O_2-scavenging catalase and GPx enzyme activities. This may increase H_2O_2 levels and therefore OH• production via the Fenton reaction, which may cause protein oxidation and induction of Hsp 70 levels (Figure 5).

The pro-oxidant effects observed in the brain 30 days after a single intravenous administration of 5 nm ceria ENM are similar to those observed in age-related or Alzheimer disease-related oxidative stress effects previously reported by our laboratory (Butterfield et al., 2001; Butterfield and Stadtman, 1997). Although all three brain regions showed an effect of 5 nm ceria ENM treatment, the extent of changes in oxidative stress indices was not same for all three brain regions. Therefore, depending upon which brain region is affected, the function of that brain region will be compromised. The EELS data suggests that mechanisms other than the valence switching between Ce^{4+} and Ce^{3+} oxidation states and the possibility to absorb and release oxygen by inducing oxygen vacancies must play a critically important role in pro-oxidant effects of ceria ENM. At present it is difficult to speculate why 5 nm ceria ENM did not cross the BBB. However, oxidative stress effects induced in brain may have been caused by some peripheral inflammatory cytokines that cross the BBB or by ROS generated as a result of long-term accumulation of 5 nm ceria ENM in peripheral organs.

Conclusions:

Although short term time exposure to ceria *in vivo* leads to a relatively small initial biochemical response (Hardas et al. 2010), ceria administration may prove to be more harmful in the long term. As reported here a single acute dose of 5 nm ceria ENM can adversely affect brain redox status after 30 d. The important point to be noted is that, ceria may induce pro-oxidant effects without crossing or disturbing BBB. The elevated oxidative stress in particular brain regions may

compromise brain functions and conceivably could even lead to neurodegeneration. Thus, implications of our study are profound for the proposed use of ceria ENM in therapeutic/non-therapeutic applications, which may lead to human exposure. Therefore, caution is suggested until and unless such effects as we demonstrated here can be mitigated.

Acknowledgements: This work was supported by United States Environmental Protection Agency Science to Achieve Results [grant number RD-833772]. Although the research described in this article has been funded wholly or in part by the United States Environmental Protection Agency through STAR Grant RD-833772, it has not been subjected to the Agency's required peer and policy review and therefore does not necessarily reflect the views of the Agency and no official endorsement should be inferred.

References:

Ahamed, M., R. Posgai, et al. (2010). "Silver nanoparticles induced heat shock protein 70, oxidative stress and apoptosis in Drosophila melanogaster." Toxicol. Appl. Pharmacol. **242**(3): 263-269.

Akhtar, M. J., M. Ahamed, et al. (2010). "Nanotoxicity of pure silica mediated through oxidant generation rather than glutathione depletion in human lung epithelial cells." Toxicology **276**(2): 95-102.

Amin, K. A., M. S. Hassan, et al. (2011). "The protective effects of cerium oxide nanoparticles against hepatic oxidative damage induced by monocrotaline." International journal of nanomedicine **6**: 143-149.

Auffan, M., J. Rose, et al. (2009). "CeO_2 nanoparticles induce DNA damage towards human dermal fibroblasts in vitro." Nanotoxicology **3**(2): 161-171.

Babu, S., J.-H. Cho, et al. (2010). "Multicolored redox active upconverter cerium oxide nanoparticle for bio-imaging and therapeutics." Chem. Commun. **46**(37): 6915-6917.

Bhabra, G., A. Sood, et al. (2009). "Nanoparticles can cause DNA damage across a cellular barrier." Nat Nano **4**(12): 876-883.

Brunner, T. J., P. Wick, et al. (2006). "In vitro cytotoxicity of oxide nanoparticles: comparison to asbestos, silica, and the effect of particle solubility." Environ. Sci. Technol. **40**(14): 4374-4381.

Butterfield, D.A., Drake, J., Pocernich, C., Castegna, A. (2001) "Evidence of oxidative damage in Alzheimer's disease brain: Central role of amyloid β-peptide." Trends Molec. Med. **7**:548-554.

Butterfield, D.A., Stadtman, E.R. (1997) "Protein oxidation processes in aging brain." Adv. Cell Aging Gerontol. **2**:161-191.

Butterfield, D. A., T. Reed, et al. (2007). "Roles of amyloid [beta]-peptide-associated oxidative stress and brain protein modifications in the pathogenesis of Alzheimer's disease and mild cognitive impairment." Free Radic. Biol. Med. **43**(5): 658-677.

Calabrese, V., T. E. Bates, et al. (2000). "NO synthase and NO-dependent signal pathways in brain aging and neurodegenerative disorders: The role of oxidant/antioxidant balance." Neurochemical Research **25**(9-10): 1315-1341.

Celardo, I., J. Z. Pedersen, et al. (2011). "Pharmacological potential of cerium oxide nanoparticles." Nanoscale **3**(4): 1411-1420.

Chen, J. P., S. Patil, et al. (2006). "Rare earth nanoparticles prevent retinal degeneration induced by intracellular peroxides." Nat. Nanotechnol. **1**(2): 142-150.

Cho, W.-S., R. Duffin, et al. (2010). "Metal oxide nanoparticles induce unique inflammatory footprints in the lung: important implications for nanoparticle testing." Environmental Health Perspectives **118**(12): 1699-1706.

Choi, J., V. Reipa, et al. (2011). "Physicochemical characterization and in vitro hemolysis evaluation of silver nanoparticles." Toxicological Sciences **123**(1): 133-143.

Colon, J., N. Hsieh, et al. (2010). "Cerium oxide nanoparticles protect gastrointestinal epithelium from radiation-induced damage by reduction of reactive oxygen species and upregulation of superoxide dismutase 2." Nanomedicine : nanotechnology, biology, and medicine **6**(5): 698-705.

D'Angelo, B., S. Santucci, et al. (2009). "Cerium oxide nanoparticles trigger neuronal survival in a human Alzheimer disease model by modulating BDNF pathway." Current Nanoscience **5**(2): 167-176.

Das, M., S. Patil, et al. (2007). "Auto-catalytic ceria nanoparticles offer neuroprotection to adult rat spinal cord neurons." Biomaterials **28**(10): 1918-1925.
Donaldson, K., V. Stone, et al. (2004). "Nanotoxicology." Occupational and Environmental Medicine **61**(9): 727-728.
Estevez, A. Y., S. Pritchard, et al. (2011). "Neuroprotective mechanisms of cerium oxide nanoparticles in a mouse hippocampal brain slice model of ischemia." Free Radic. Biol. Med. **51**(6): 1155-1163.
Fubini, B., M. Ghiazza, et al. (2010). "Physico-chemical features of engineered nanoparticles relevant to their toxicity." Nanotoxicology **4**(4): 347-363.
Gilliss, S. R., J. Bentley, et al. (2005). "Electron energy-loss spectroscopic study of the surface of ceria abrasives." Applied Surface Science **241**(1-2): 61-67.
Guo, Y.-Y., J. Zhang, et al. (2011). "Cytotoxic and genotoxic effects of multi-wall carbon nanotubes on human umbilical vein endothelial cells in vitro." Mutation Research/Genetic Toxicology and Environmental Mutagenesis **721**(2): 184-191.
Halliwell, B. (1992). "Reactive oxygen species and the central-nervous-system." J. Neurochem. **59**(5): 1609-1623.
Hao, L., Z. Wang, et al. (2009). "Effect of sub-acute exposure to TiO_2 nanoparticles on oxidative stress and histopathological changes in Juvenile Carp (Cyprinus carpio)." Journal of Environmental Sciences **21**(10): 1459-1466.
Hardas, S. S., D. A. Butterfield, et al. (2010). "Brain distribution and toxicological evaluation of a systemically delivered engineered nanoscale ceria." Toxicological Sciences **116**(2): 562-576.
Hirst, S. M., A. Karakoti, et al. (2011). "Bio-distribution and in vivo antioxidant effects of cerium oxide nanoparticles in mice." Environmental Toxicology: n/a-n/a.
Hirst, S. M., A. S. Karakoti, et al. (2009). "Anti-inflammatory Properties of Cerium Oxide Nanoparticles." Small **5**(24): 2848-2856.
Hissin, P. J. and R. Hilf (1976). "A fluorometric method for determination of oxidized and reduced glutathione in tissues." Analytical Biochemistry **74**(1): 214-226.
Korsvik, C., S. Patil, et al. (2007). "Superoxide dismutase mimetic properties exhibited by vacancy engineered ceria nanoparticles." Chem. Commun.(10): 1056-1058.
Landsiedel, R., M. D. Kapp, et al. (2009). "Genotoxicity investigations on nanomaterials: Methods, preparation and characterization of test material, potential artifacts and limitations—Many questions, some answers." Mutation Research/Reviews in Mutation Research **681**(2-3): 241-258.
Liang, G., Y. Pu, et al. (2009). "Influence of Different Sizes of Titanium Dioxide Nanoparticles on Hepatic and Renal Functions in Rats with Correlation to Oxidative Stress." J Toxicol Environ Health A **72**(11-12): 740-745.
Lin, W. S., Y. W. Huang, et al. (2006). "Toxicity of cerium oxide nanoparticles in human lung cancer cells." Int. J. Toxicol. **25**(6): 451-457.
Mocan, T., S. Clichici, et al. (2010). "Implications of oxidative stress mechanisms in toxicity of nanoparticles (review)." Acta Physiologica Hungarica **97**(3): 247-255.
Nakagawa, Y., T. Suzuki, et al. (2011). "Cytotoxic effects of hydroxylated fullerenes on isolated rat hepatocytes via mitochondrial dysfunction." Arch. Toxicol. **85**(11): 1429-1440.
Nel, A., T. Xia, et al. (2006). "Toxic potential of materials at the nanolevel." Science **311**(5761): 622-627.

Nesic, O., G.-Y. Xu, et al. (2004). "IL-1 Receptor Antagonist Prevents Apoptosis and Caspase-3 Activation after Spinal Cord Injury " Journal of Neurotrauma **18**(9): 947-956.
Niu, J., A. Azfer, et al. (2007). "Cardioprotective effects of cerium oxide nanoparticles in a transgenic murine model of cardiomyopathy." Cardiovascular Research **73**(3): 549-559.
Niu, J., K. Wang, et al. (2011). "Cerium Oxide Nanoparticles Inhibits Oxidative Stress and Nuclear Factor-κB Activation in H9c2 Cardiomyocytes Exposed to Cigarette Smoke Extract." J. Pharmacol. Exp. Ther. **338**(1): 53-61.
Park, E. J., J. Choi, et al. (2008). "Oxidative stress induced by cerium oxide nanoparticles in cultured BEAS-2B cells." Toxicology **245**(1-2): 90-100.
Pigeolet, E., P. Corbisier, et al. (1990). "Glutathione-peroxidase, superoxide-dismutase, and catalase inactivation by peroxides and oxygen derived free-radicals." Mechanisms of Ageing and Development **51**(3): 283-297.
Pirmohamed, T., J. M. Dowding, et al. (2010). "Nanoceria exhibit redox state-dependent catalase mimetic activity." Chem. Commun. **46**(16): 2736-2738.
Radu, M., M. C. Munteanu, et al. (2010). "Depletion of intracellular glutathione and increased lipid peroxidation mediate cytotoxicity of hematite nanoparticles in MRC-5 cells." Acta Biochemica Polonica **57**(3): 355-360.
Rahman, M. F., J. Wang, et al. (2009). "Expression of genes related to oxidative stress in the mouse brain after exposure to silver-25 nanoparticles." Toxicology Letters **187**(1): 15-21.
Rzigalinski, B. A., K. Meehan, et al. (2006). "Radical nanomedicine." Nanomedicine (Lond) **1**(4): 399-412.
Sharma, H. S. and A. Sharma (2007). Nanoparticles aggravate heat stress induced cognitive deficits, blood–brain barrier disruption, edema formation and brain pathology. Progress in Brain Research, Elsevier. **162:** 245-273.
Srinivas, A., P. J. Rao, et al. (2011). "Acute inhalation toxicity of cerium oxide nanoparticles in rats." Toxicology Letters **205**(2): 105-115.
Sultana, R., M. Piroddi, et al. (2008). "Protein Levels and Activity of Some Antioxidant Enzymes in Hippocampus of Subjects with Amnestic Mild Cognitive Impairment." Neurochem Res **33**(12): 2540-2546.
Tangpong, J., M. P. Cole, et al. (2006). "Adriamycin-induced, TNF-α-mediated central nervous system toxicity." Neurobiology of Disease **23**(1): 127-139.
Usenko, C. Y., S. L. Harper, et al. (2008). "Fullerene C60 exposure elicits an oxidative stress response in embryonic zebrafish." Toxicol. Appl. Pharmacol. **229**(1): 44-55.
Wang, J., M. F. Rahman, et al. (2009). "Expression changes of dopaminergic system-related genes in PC12 cells induced by manganese, silver, or copper nanoparticles." NeuroToxicology **30**(6): 926-933.
Wang, J., P. Sun, et al. (2011). "Cytotoxicity of single-walled carbon nanotubes on PC12 cells." Toxicol. Vitro **25**(1): 242-250.
Xia, T., M. Kovochich, et al. (2008). "Comparison of the mechanism of toxicity of zinc oxide and cerium oxide nanoparticles based on dissolution and oxidative stress properties." Acs Nano **2**(10): 2121-2134.
Xia, T., N. Li, et al. (2009). "Potential health impact of nanoparticles." Annual Review of Public Health **30**(1): 137-150.
Xiong, D., T. Fang, et al. (2011). "Effects of nano-scale TiO_2, ZnO and their bulk counterparts on zebrafish: Acute toxicity, oxidative stress and oxidative damage." Science of The Total Environment **409**(8): 1444-1452.

Yokel, R. A., R. L. Florence, et al. (2009). "Biodistribution and oxidative stress effects of a systemically-introduced commercial ceria engineered nanomaterial." Nanotoxicology **3**(3): 234-248.

Yokel, R. A., R. L. Florence, et al. (2009). "Biodistribution and oxidative stress effects of a systemically-introduced commercial ceria engineered nanomaterial." Nanotoxicology **3**(4): 234-248.

Younce, C. W., K. Wang, et al. (2010). "Hyperglycaemia-induced cardiomyocyte death is mediated via MCP-1 production and induction of a novel zinc-finger protein MCPIP." Cardiovascular Research **87**(4): 665-674.

Zhou, X., L. L. Wong, et al. (2011). "Nanoceria inhibit the development and promote the regression of pathologic retinal neovascularization in the vldlr knockout mouse." PLoS ONE **6**(2): e16733.

Table legend:

Table 1: Cerium concentrations in blood, brain, and liver, expressed as concentration and as a percentage of the ceria ENM dose. [Ce] in mg/kg wet weight of the blood or tissue (mean ± SD).

Table 1: Cerium concentrations in blood, brain, and liver

Cerium concentration [Ce] (mg/kg) wet weight and as a % of the ceria ENM dose[a]			
	Blood (mg/kg)	**Brain (mg/kg)**	**Liver (mg/kg)**
[Ce]	0.11 ± 0.16	0.38 ± 0.52	505 ± 238
% dose	0.01 ± 0.02	0.008 ± 0.009	44 ± 27

[a] Based on reference volume of blood in the rat (7% of body weight) or weight of the brain or liver times the ceria concentration.

Figure legends:

Figure 1: Ceria ENM imaged using HRTEM. The ceria were dispersed on a carbon film. Visually they have a narrow size distribution ranging from 4 to 6 nm, the majority 5 nm.

Figure 2: In hippocampus 30 d after a single acute dose of 5 nm ceria ENM: **a**) histograms showing GR, GPx, catalase, antioxidant enzymes and Hsp70 heat shock protein levels and corresponding Western blot experiments showing protein levels in control [C] and treated [T] samples. The intensity of each band was normalized with intensity of corresponding band of β-actin-loading control (not shown); **b**) GR, GPx catalase antioxidant activities, and GSH: GSSG ratio measured in control and ceria treated samples; and **c**) oxidative stress markers PC, 3NT and HNE levels. The values are calculated as % control for each measurement expressed as mean ± SEM, control n = 7, treated n = 9, *p <0.05, **p < 0.01, compared to control.

Figure 3: In cortex 30 d after a single acute dose of 5 nm ceria ENM: **a**) histograms showing GR, GPx, catalase, antioxidant enzymes and Hsp70 heat shock protein levels and corresponding Western blot experiments showing protein levels in control [C] and treated [T] samples. The intensity of each band was normalized with intensity of corresponding band of β-actin-loading control (not shown); **b**) GR, GPx, catalase, antioxidants activities and GSH: GSSG ratio measured in control and ceria treated samples; **c**) oxidative stress markers PC, 3NT and HNE levels, and **d**) iNOS levels and correlation between 3NT levels and iNOS levels in ceria treated samples, n=9, r=0.67, p < 0.05. The values are calculated as % control for each measurement expressed as mean ± SEM, control n = 7, treated n = 9, *p <0.05, **p < 0.01, compared to control.

Figure 4: In cerebellum 30 d after a single acute dose of 5 nm ceria ENM: **a**) histograms showing GR, GPx, catalase, antioxidant enzymes and Hsp70 heat shock protein levels and

corresponding Western blot experiments showing protein levels in control [C] and treated [T] samples. The intensity of each band was normalized with intensity of corresponding band of β-actin-loading control (not shown); **b**) GR, GPx, catalase, antioxidants activities, and GSH: GSSG ratio measured in control and ceria treated samples, and **c**) oxidative stress markers PC, 3NT and HNE levels. The values are calculated as % control for each measurement expressed as mean ± SEM, control n = 7, treated n = 8, *p <0.05, **p < 0.01, compared to control.

Figure 5: In this proposed pathway ceria ENM induces pro-oxidant effects on rat brain without crossing BBB. Ceria ENM indirectly induces ROS production leading to GSH depletion and inhibition of catalase and GPx enzymes. This inhibition of H_2O_2 reducing enzyme activity can induce H_2O_2 levels and therefore hydroxyl radicals (OH•) production mediated by Fenton reaction. Increased OH• can further oxidize the proteins and may hamper their regular function. Hydroxyl radicals may also inhibit H_2O_2 reducing catalase and GPx activity by way of oxidative modification. These biochemical reactions could make cellular environment more oxidizing, triggering a cellular stress response to induce Hsp-70 levels. Hsp-70 is a chaperone protein that can shepherd oxidized proteins to the 20S proteosome for degradation for further cellular clearance (shown as dotted arrow). If timely clearance of oxidized protein takes place then there may not be any change in cellular PC levels. As there was no evidence of the presence of ceria ENM inside the brain, it is further proposed that ceria ENM exert their pro-oxidant effect in the brain secondary to its peripheral effects.

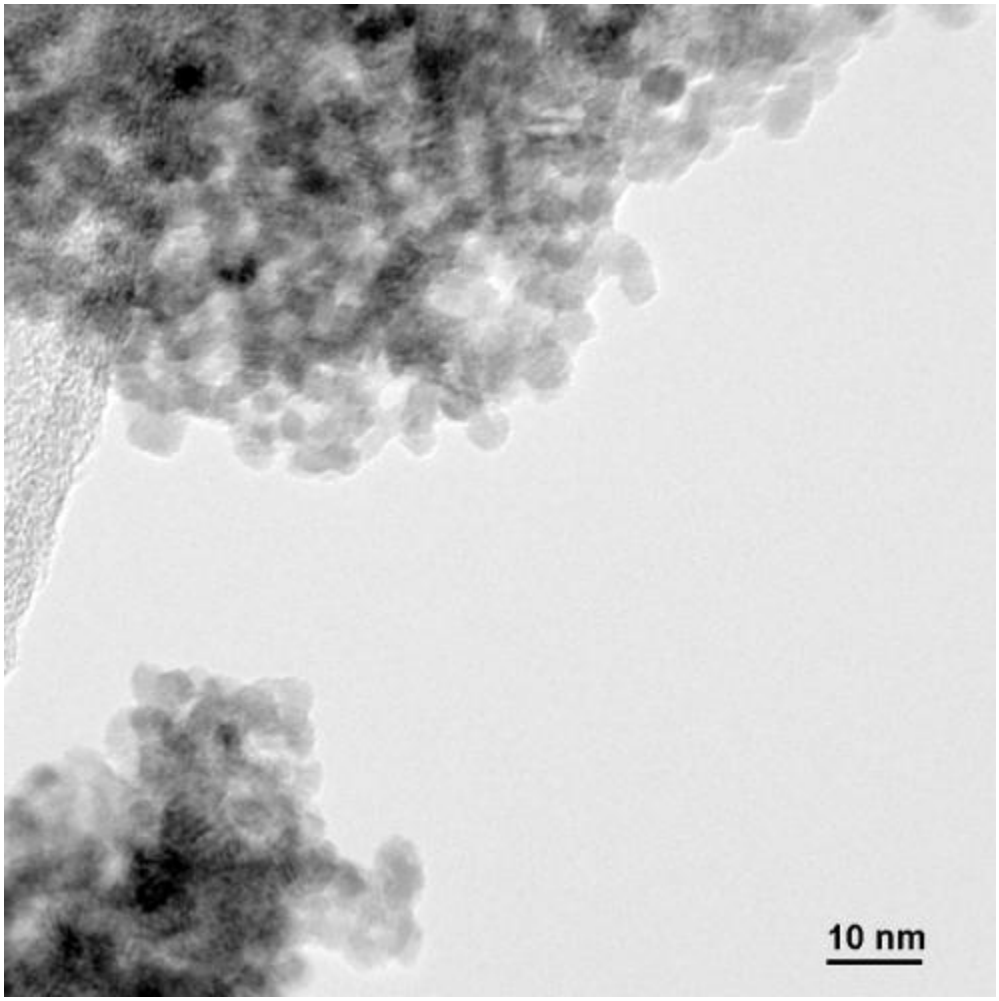
10 nm

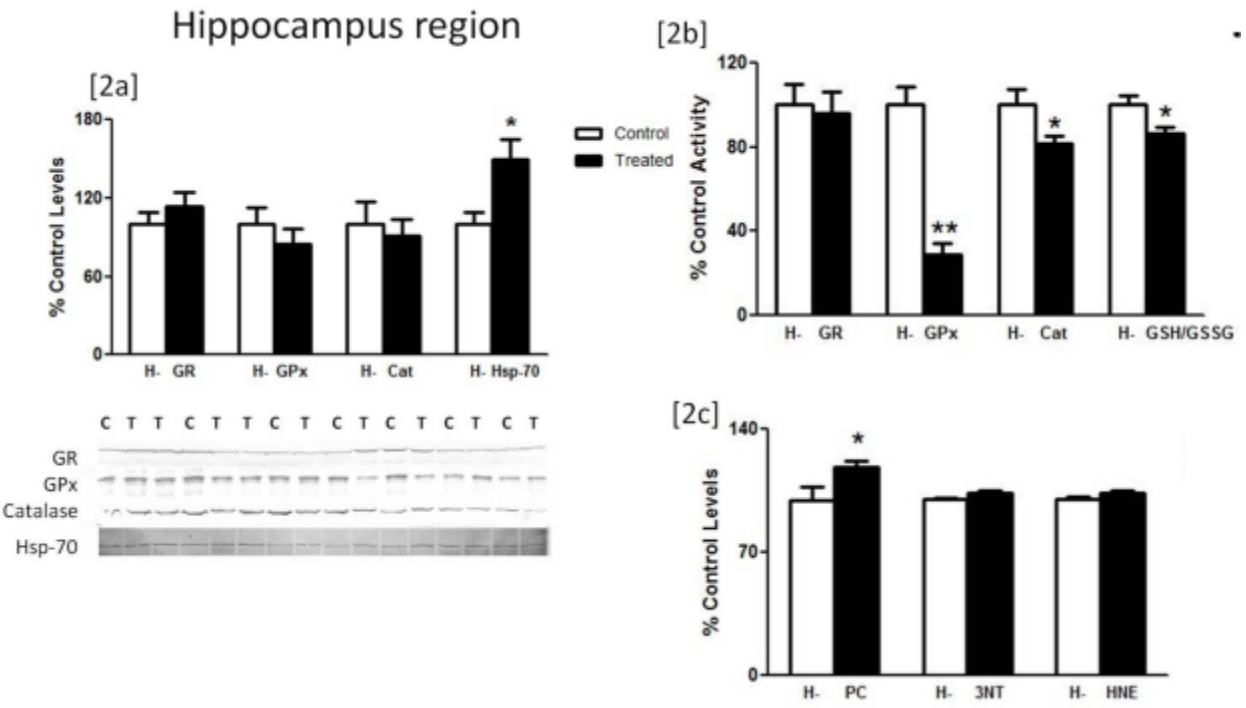
Hippocampus region
[2a]
% Control Levels
180
120
60
0
H- GR
H- GPx
H- Cat
H- Hsp-70
C T T C T T C T C T C T C T C T
GR
GPx
Catalase
Hsp-70
Control
Treated
[2b]
% Control Activity
120
80
40
0
H- GR
H- GPx
H- Cat
H- GSH/GSSG
[2c]
% Control Levels
140
70
0
H- PC
H- 3NT
H- HNE

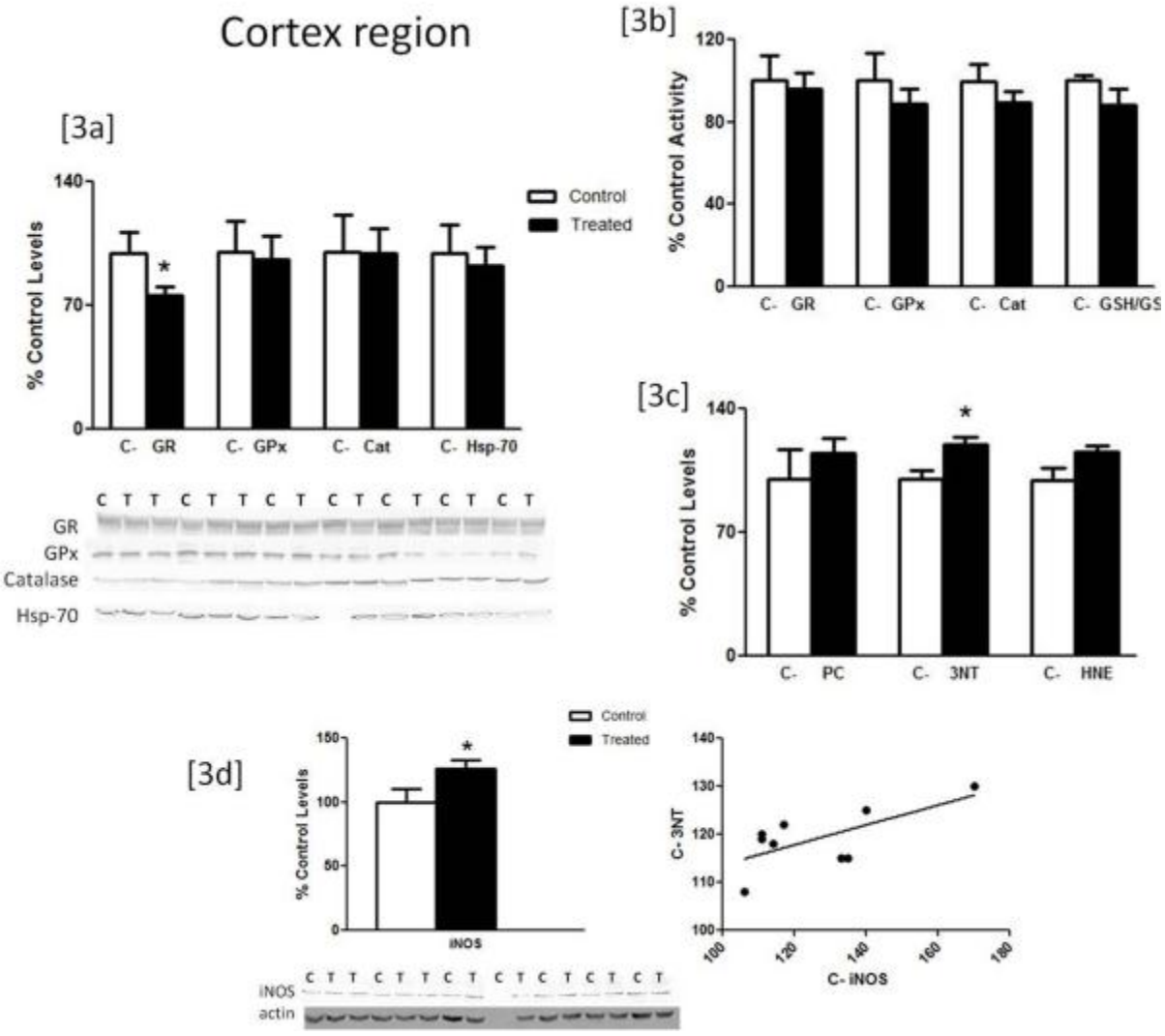
Cortex region
[3a]
% Control Levels
140
70
0
Control
Treated
*
C- GR
C- GPx
C- Cat
C- Hsp-70
C T T C T T C T C T C T C T C T
GR
GPx
Catalase
Hsp-70
[3b]
% Control Activity
120
80
40
0
C- GR
C- GPx
C- Cat
C- GSH/GS
[3c]
% Control Levels
140
70
0
*
C- PC
C- 3NT
C- HNE
[3d]
Control
Treated
% Control Levels
150
100
50
0
*
iNOS
C T T C T T C T C T C T C T C T
iNOS
actin
C- 3NT
140
130
120
110
100
100
120
140
160
180
C- iNOS

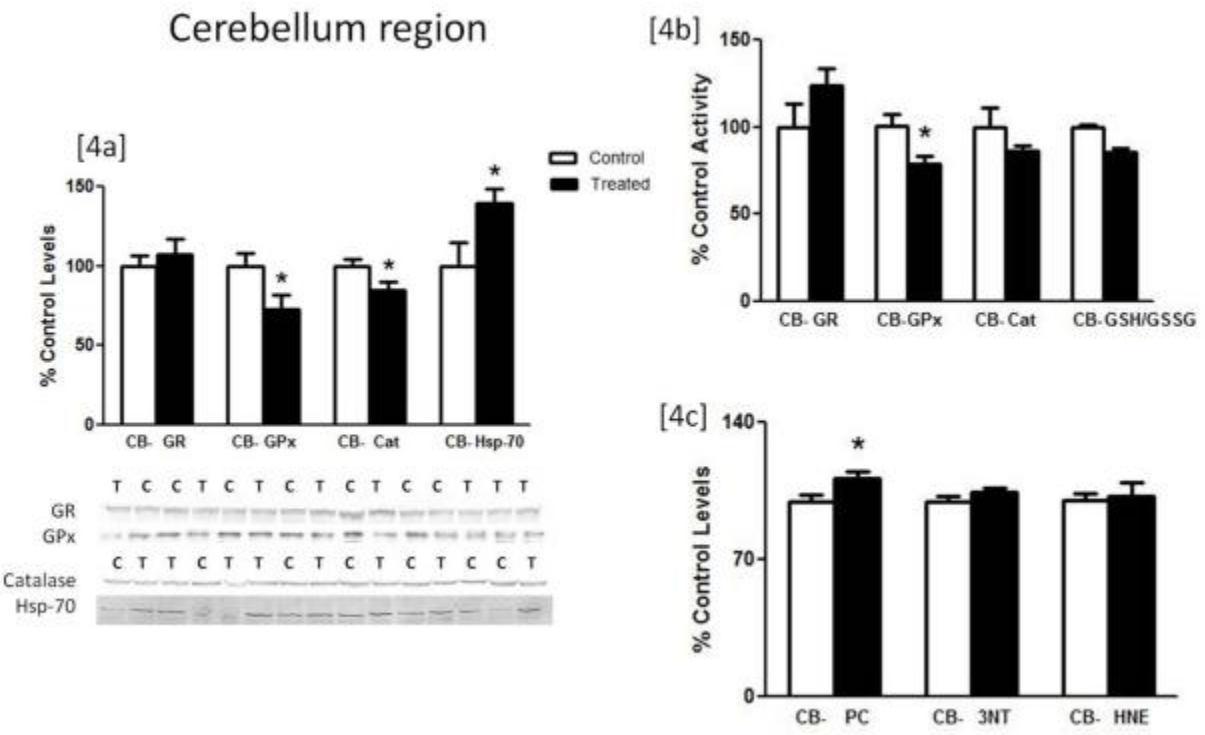
Cerebellum region
[4a]
Control
Treated
% Control Levels
150
100
50
0
CB- GR
CB- GPx
CB- Cat
CB- Hsp-70
T C C T C T C T C T C C T T T
GR
GPx
C T T C T T C T C T C T C C T
Catalase
Hsp-70
[4b]
% Control Activity
150
100
50
0
CB- GR
CB-GPx
CB- Cat
CB-GSH/GSSG
[4c]
% Control Levels
140
70
0
CB- PC
CB- 3NT
CB- HNE

1

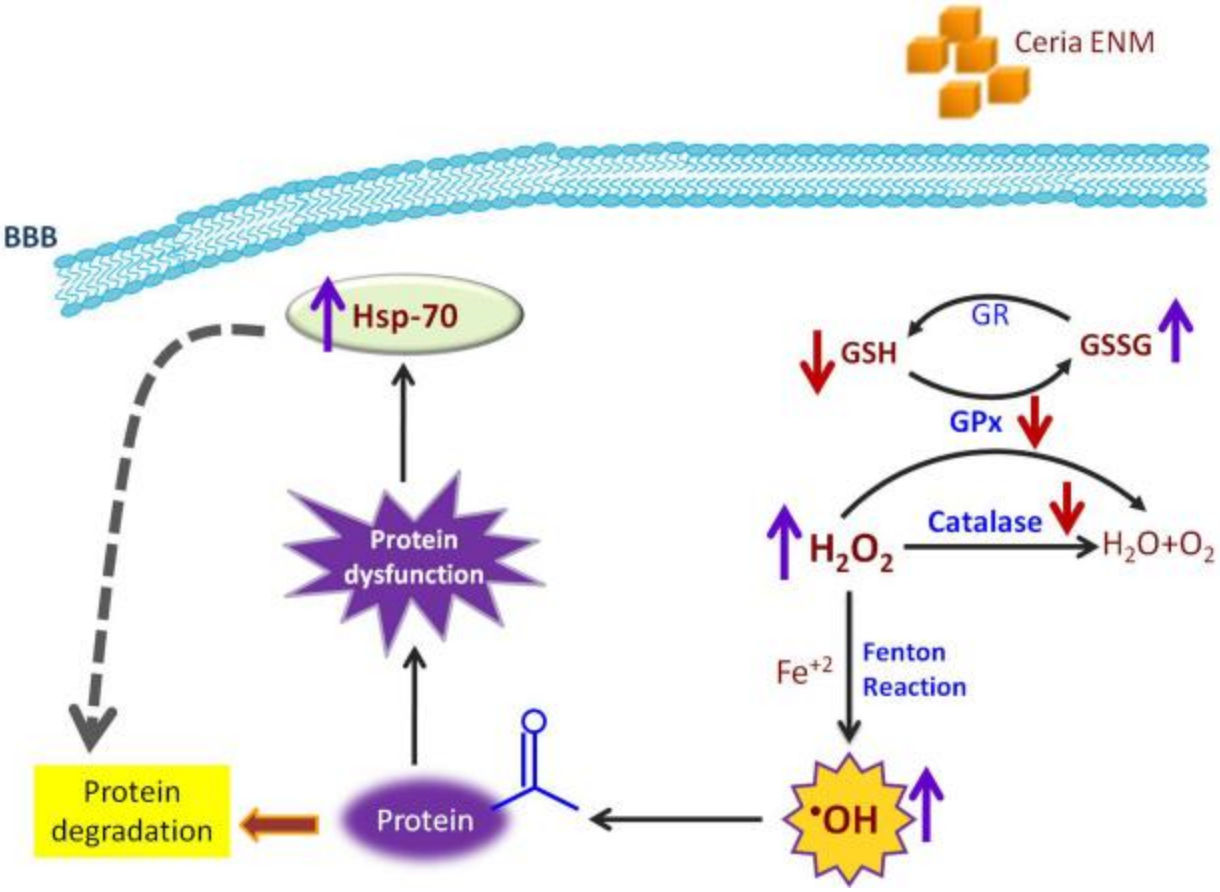
Ceria ENM
BBB
Hsp-70
Protein dysfunction
GR
GSH
GSSG
GPx
Catalase
H_2O_2
H_2O+O_2
Fe^{+2}
Fenton Reaction
•OH
Protein
Protein degradation

2